COMPARISON OF SATELLITE IMAGE DENOISING TECHNIQUES IN SPATIAL AND FREQUENCY DOMAINS

S. Oguzhanoglu*, I. Kapucuoglu, F. Sunar

ITU, Civil Engineering Faculty, 80626, Maslak Istanbul, Turkey - (oguzhanoglu17, kapucuoglu17, fsunar)@itu.edu.tr

Commission III, ICWG III/IVb

KEY WORDS: Noise, Denoising, Optical Satellite Images, Wavelet-based Contourlet Transform, Curvelet Transform, Block Matching and 3D Filtering, Median Filter.

ABSTRACT:

In recent years, remote sensing images have been used for many different applications that require visual analysis and interpretation. In this paper, reducing/removing noise is the basic approach, as it causes loss of information and therefore affects the accuracy of the analyses. Within the scope of the study, two different test areas of land cover/use were applied to examine the effects of noise on optical satellite images. In this context, Landsat 8 and Sentinel 2 satellites were used to study the effects of denoising methods on different spatial resolutions. Due to the lack of raw images of the selected satellites, two different types of noise (i.e. Gaussian and Stripe) were added to the images. In this context, four different denoising methods were compared by using conventional filter techniques commonly used in the spatial domain, while also different methods that used different threshold values in the frequency domain. The first approach is Median, Block Matching and 3D Filtering methods in the spatial domain, applications that depend mainly on the neighborhood relationship of pixels in the image. The second approach is wavelet-based Contourlet and Curvelet methods in the frequency domain. The quality analysis of denoised images were evaluated as qualitative (statistical methods Peak Signal to Noise Ratio, Mean Square Error, standard deviation, min/max value), and quantitative. Finally, Curvelet hard thresholding transform was the selected method as the best algorithm after quality analysis additionally, the method also effectively preserves edges in homogeneous test area and other fine details in the heterogeneous test area.

1. INTRODUCTION

Nowadays, remote sensing has become an effective technique for monitoring and extracting information about Earth features from a distance. In addition, this developing technology contributes much more to new scientific studies for humanity by providing a high level of detailed information and accuracy. However, despite the rapid technological development, there are still limitations in the image acquisition and transfer steps, so some image distortions may occur.

Pre-processing, which is the first step in the analysis of satellite images used in different applications, is a very important step and must be done carefully. In other words, some distortions need to be corrected before applying analysis and post-processing techniques to improve image quality. In general, pre-processing techniques include radiometric correction (for distortions caused by sensor characteristics and differences in illumination conditions), atmospheric correction (for distortions caused by atmospheric interactions with particles such as clouds and aerosols in the atmosphere), and geometric correction (for distortions caused by altitude, sensor, or earth variations, etc.).

One of the main radiometric errors caused by sensor is “noise” and needs to be reduced as it causes poor image quality, loss of information, and low accuracy analysis. Noises are often seen as systematic (i.e. striping/banding) and random (i.e. Gaussian). For example, drop lines during scanning, gaps in the scan forward and backward, and calibration changes between sensor systems in multi-sensor detectors are the main causes of band striping (Tsai and Chen, 2008). Also, noise depends on the high-frequency content of the image; therefore, there must be a balance between reducing and suppressing noise in an image as much as possible without losing too much information.

Denoising has always been a critical issue in image processing; therefore, various approaches developed depending on the statistical properties of noise (i.e. low frequency and high frequency) are classified as techniques used in the spatial and frequency domains. In the spatial domain, operations are based on the brightness value of the pixel (i.e. grey value) and the neighbor relations, while in the frequency domain, operations depend on the frequency and temporal change information of the values defined in the time and spatial domain (Ruikar and Dove, 2011).

In the literature review of the methods used in noise removal (i.e. denoising), it was seen that the techniques were most commonly developed not for satellite images, but rather by using test images such as "Lena", "Barbara". Due to this mentioned shortcoming, optical remote sensing data (Sentinel 2 and Landsat 8) were used to test the denoising performances in two different test areas in this study. For this purpose, four different methods were applied in two different and tested and the best one was selected by comparing their image quality performance.

For this purpose, four different methods (Median Filtering, Block Matching and 3D Filtering (BM3D), Curvelet Transform, Wavelet-based Contourlet Transform) were applied and tested in two different domains (frequency and spatial), then the image quality performance measures were compared and most appropriate one for each domain was selected.

2. STUDY AREA & DATA USED

2.1 Study Area

Istanbul is the most important city in Turkey with rapid urbanization in the northwest of Turkey, which connects the

* The corresponding author.

Black Sea to the Mediterranean Sea via the Sea of Marmara. The reason why the two study areas were chosen in Istanbul is that it has very complex heterogeneous areas such as agricultural areas, artificial surfaces, and homogeneous areas such as forest areas and water areas. In this context, the homogeneous test area was chosen in the Çatalca region, which includes predominantly forested areas and where the land cover/use does not change much, and the heterogeneous test area with different land cover/use classes around Alibeyköy (Figure 1).

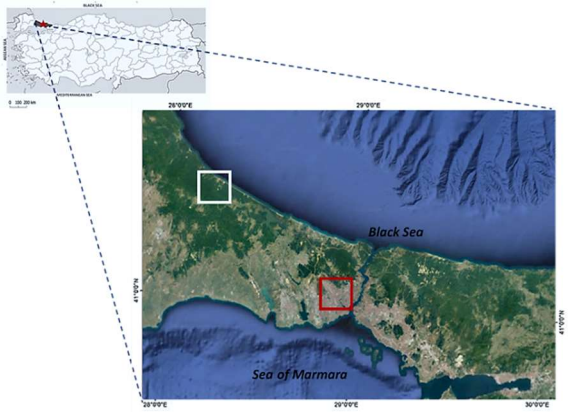

Figure 1. Satellite image of two test areas in Istanbul – Çatalca (white box) and Alibeyköy (red box) (©2020, Google Earth).

2.2 Data Used

For denoising analysis, the selected methods were applied on Landsat 8/OLI and Sentinel-2B/MSI satellites images dated July 1, 2020. The same acquisition date of the two satellites makes this study even more remarkable as it will make a significant contribution to the evaluation of the effects of different spatial resolutions on the performance of denoising techniques.

Landsat 8 carries OLI (Operational Land Imager), and Sentinel 2 carries Multispectral Instrument (MSI). The characteristics of the two satellite bands are given in Table 1. For this study, the blue (B2), green (B3) and red (B4) bands of both satellites were used. Besides, panchromatic (PAN – B8) band of the Landsat 8 satellite was used.

Landsat 8/OLI			Sentinel 2/MSI		
Band	Spectral Res. (µm)	Spatial Res. (m)	**Band**	Spectral Res. (µm)	Spatial Res. (m)
B1	0.443	30	**B1**	0.443	60
B2	0.483	30	**B2**	0.490	10
B3	0.560	30	**B3**	0.560	10
B4	0.660	30	**B4**	0.665	10
			B5	0.705	20
			B6	0.740	20
			B7	0.783	20
B5	0.865	30	**B8**	0.842	10
			B8A	0.865	20
			B9	0.945	60
B6	1.650	30	**B11**	1.375	20
B7	2.220	30	**B12**	1.610	20
B9	1.375	30	**B10**	2.190	60
B8	0.640	15			

Table 1. Landsat-8 and Sentinel-2 spectral band properties.

3. METHODOLOGY

Image errors, for example that cause distortion or unwanted data, are known as noise. For satellite images, the most common ones are stripe and random (i.e. Gaussian) noises. Besides, denoising images that have been distorted by Gaussian noise is a typical signal processing issue (Ruikar and Dove, 2011; Luisier et al., 2007). Since the Level-0 (raw) images of the dataset used in this study could not be accessed, two common noise types were added to the satellite images using Eq. (1).

$$Y_n = X_n + b_n \quad (1)$$

where; Y_n = Noisy data
X_n = Original satellite image
b_n = Noise (Gaussian or stripe)

Denoising for satellite images is a more complex and variable process as the noise affecting the image may be diverse for different land use/cover. In addition, in low and high spatial frequency areas (i.e. forest and urban) in satellite images, low-frequency noise is more difficult to distinguish as it usually has a similar structure (i.e. grey value) to the original data in the images (Vijay and Devi, 2012). For this reason, methods are generally developed to remove low-frequency noise.

To evaluate the performance of the denoising process, four different methods were applied in two different domains (i.e. spatial and frequency) to the selected test areas in both satellite images. These methods are Median (using different kernel sizes (i.e. 3x3 and 5x5)) and BM3D (using different noise standard deviation parameters (i.e. σ= 0.2, 0.4)) algorithms in the spatial domain and Curvelet (using different threshold (i.e. hard and soft)) and wavelet-based Contourlet transforms in the frequency domain.

The processing steps applied to determine the denoising performance are given in Figure 2.

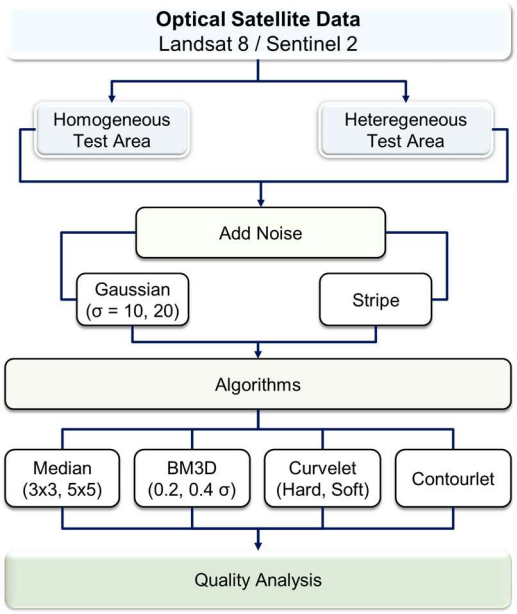

Figure 2. Flow chart used for the study.

The methods are used in the study are briefly explained in the following sub-sections.

3.1 Denoising algorithms in the spatial domain

In general, the filtering methods used in the spatial domain are based on the use of statistical parameters of the image (min, max, median, etc.) and minimize low-frequency noise while preserving important features (i.e. fine details, edges) in the image (Yu et al., 2009).

3.1.1 Median filter: Median filter is a method based on the statistical properties of the image. The output of Median filter is a median value of all values in the kernel; after filtering, the center pixel value is changed with the median value (Ahmed et al., 2015). Since it is not affected by the lowest or highest pixel value, the Median filter is suitable for denoising; however, the image loses edge sharpness and becomes soft (Sunar et al., 2017).

3.1.2 BM3D: The BM3D algorithm is based on block matching, a collaborative filter (i.e. Wiener), and thresholding (i.e. hard threshold) (Dabov et al., 2007). The processing step begins with grouping the pixels depends on their similarity and filtering is done on each group of blocks. Following the filtering process, Wiener filtering is performed, and then with the inverse transform, a denoised image is obtained. Besides, the BM3D algorithm protects sharpness, homogeneous areas, and edges in practice (Lebrun, 2012).

3.2 Denoising algorithms in the frequency domain

Earlier, denoising was done in the frequency domain using linear methods such as the Fourier transform. However, due to the difficulty to handle non-linear structures, wavelet-based techniques that include operations such as thresholding in the frequency domain have been developed (Naveed et al., 2019). Considering their simplicity and efficiency, wavelet-based (such as discrete, complex, continuous wavelet transforms) algorithms in the frequency domain continue to be useful for denoising. However, methods in the frequency domain are generally more complex and have more time-consuming processing steps than the methods performed in the spatial domain.

3.2.1 Curvelet transform: Curvelet is a multiscale transform similar to wavelet transform, with structural components ordered by location parameters and scale. When the transform is applied with different threshold values (i.e. hard and soft), it effectively softens the image while preserving fine details in the image (Nencini et. al., 2007).

3.2.2 Contourlet transform: Wavelet-based Contourlet is a transform based on the Laplacian pyramid and directional filter bank that enables the creation of images to have contours with multi-scale and multi-direction (i.e. different scales and directions) (Do and Vetterli, 2006). In this way, the detail of the images is preserved and the sharpness of the edges is ensured (Altun and Allahverdi, 2007).

3.3 Quality Analysis

Quality analysis should be able to detect and measure distortions in the image, in order to preserve or improve image quality (Wang and Bovik, 2006). The first-order metrics of image quality analysis (e.g. standard deviation, variance) allow interpretation for pixels of the image (i.e. statistical behavior). In addition, second-order metrics (i.e. PSNR and MSE) that take into account the spatial relationship properties of two pixels comparative to each other are crucial (Rajkumar and Malathi, 2016).

PSNR is defined as in the Eq. (2).

$$PSNR = 10\ log_{10} \frac{Max\ Pixel\ Value^2}{MSE} \quad (2)$$

4. APPLICATION & RESULTS

4.1 Add Noise

Since the selected satellite images are not raw (i.e. unprocessed) data, the two most common types of noise in applications; Gaussian noise with σ=10 and σ=20 were added on panchromatic (PAN), blue, green, red bands and stripe noise were added on PAN (Figure 3). As seen, when the sigma values increase, the noise ratio in the image also increases.

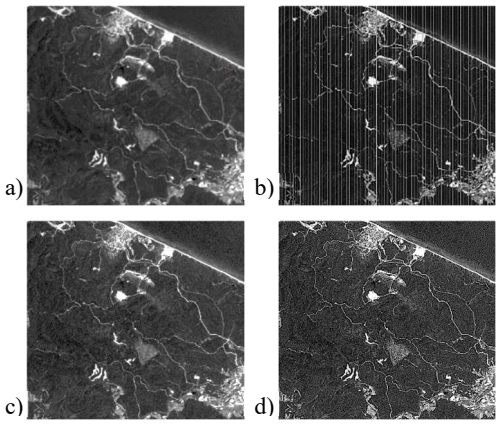

Figure 3. Example of Gaussian and stripe noise in homogeneous test area. (a) Landsat 8/Band 8 Panchromatic image, (b) Stripe noise, (c) σ=10 Gaussian noise, (d) σ=20 Gaussian noise.

4.2 Gaussian noise denoising in the spatial domain

As shown in Figure 4, both algorithms, tested on different satellites with different spatial resolutions, caused image details to become smoother.

In the Median filter, which is the conventional method for image denoising in the spatial domain, the effect of kernel selection on noise removal was tested, and as expected, it was observed that the smoothing effect on images increased as the kernel size increased (i.e. 5x5, Figure 4(b)). It can be said that the Median filter with a 3x3 kernel works better and more effective in terms of preventing loss of information (Figure 4(a)). This effect can be seen visually by comparing the homogeneous areas (i.e. water) and heterogeneous areas (i.e. the areas outside the urban areas) in both satellite images.

On the other hand, in BM3D method, as the sigma value increases, it was observed that the smoothing effect occurs more which causing information loss (Figure 4(d)). Due to the low resolution of Landsat 8 images, it was observed that some linear structures were significantly removed in both heterogeneous (e.g. buildings) and homogeneous areas (e.g. roads) (Figure 4.2(d)).

Although, the BM3D method is common and new developed algorithm in image processing, especially in medical applications, it was observed that the method did not work well on the satellite images. This can be explained by the complexity of the images, which contain a lot of information in the form of features based on different spatial, frequency and spectral characteristics.

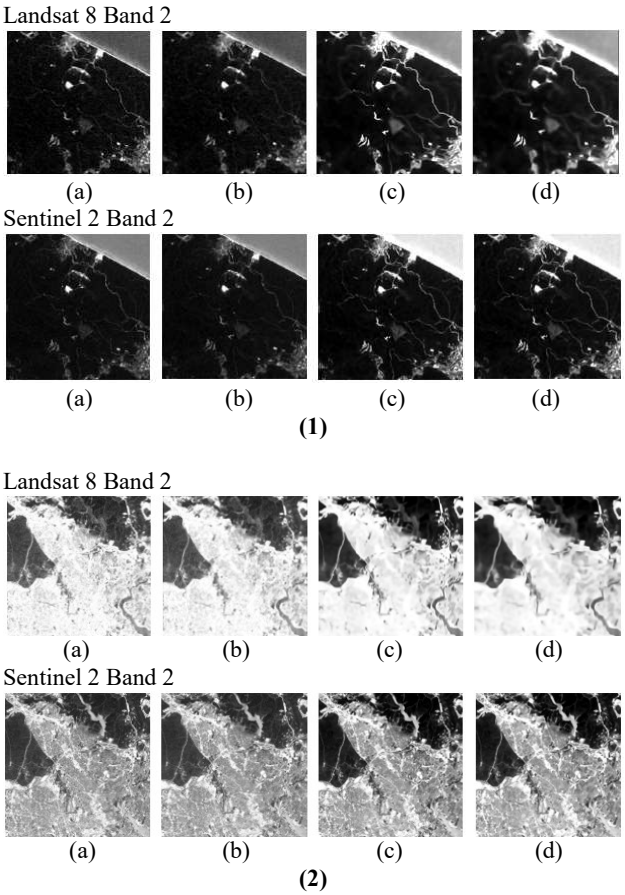

Figure 4. Denoised images of test areas on Landsat 8 and Sentinel 2 images for (1) homogeneous and (2) heterogeneous areas; (a) Median 3x3 filter, (b) Median 5x5 filter, (c) σ=0.2 BM3D, (d) σ=0.4 BM3D.

The statistical analysis of the denoised Landsat images is shown in Table 2. As higher PSNR value and lower MSE value mean better image quality, therefore, the use of 3x3 Median filter at low noise level (σ=10) gave better results in both satellites. Table 2.

In the spatial domain, it was concluded that the denoising results Median filter with a 3x3 kernel gave visually and statistically better results, especially in detail preservation.

4.3 Gaussian noise denoising in the frequency domain

First, in Curvelet transform, PSNR-threshold value plot was produced to separately select the best threshold value for soft and hard thresholding, and then the transformed images were generated after choosing the best threshold value for each. The selection of the best value (i.e. 1.2) for the hard threshold and the transform image are given in Figure 5 as an example.

Afterwards, denoising was performed with soft and hard thresholding value selection. The denoised images of test areas on Landsat 8 and Sentinel 2 images for homogeneous and heterogeneous areas are given in Figure 6. One of the main problems detected was that there were some artifacts for Gaussian noise in both images, but this issue was less pronounced with soft thresholding than with hard one. However, denoising has caused information loss in heterogeneous test areas, especially in urban areas (Figure 6.2(a)).

On the other hand, in the Contourlet transform, first the transform image was produced with subbands (Figure 7(a)) for the images with Gaussian noise. It was observed that reconstructed images denoised with the Contourlet transform gave less smoothing effect than Curvelet transform. However, artifacts similar to those in the Curvelet transform were excessive in this transformation, resulting in more information loss (especially observed in forest areas in the heterogeneous and homogeneous test areas).

The statistical analysis of the denoising methods in the frequency domain is shown in Table 3. As seen, Curvelet transform with hard thresholding was chosen as the best method in the frequency domain statistically (i.e. with its highest PSNR values).

Sentinel 2	PSNR			MSE		
	B2	B3	B4	B2	B3	B4
σ=10 Gaussian Noise						
Median 3x3	**27.11**	**26.75**	**27.18**	**126.54**	**137.42**	**124.43**
Median 5x5	24.97	24.52	24.61	207.06	229.39	224.71
BM3D 0.2	12.79	12.08	14.10	3420.42	4027.48	2531.97
BM3D 0.4	12.79	12.08	14.09	3421.61	4028.40	2532.85
σ=20 Gaussian Noise						
Median 3x3	**23.05**	**22.24**	**23.11**	**322.39**	**387.81**	**317.88**
Median 5x5	22.06	21.27	21.91	404.67	485.05	418.94
BM3D 0.2	12.50	11.80	13.71	3660.21	4297.65	2764.89
BM3D 0.4	12.49	11.80	13.71	3661.37	4298.56	2765.78

(a)

Sentinel 2	PSNR			MSE		
	B2	B3	B4	B2	B3	B4
σ=10 Gaussian Noise						
Median 3x3	**22.47**	**22.61**	**23.04**	**368.54**	**356.9**	**322.82**
Median 5x5	19.61	19.75	19.98	710.61	689.29	653.58
BM3D 0.2	4.20	4.38	4.48	24729.20	23726.86	23161.88
BM3D 0.4	4.20	4.38	4.48	24726.35	23721.79	23160.40
σ=20 Gaussian Noise						
Median 3x3	**20.23**	**20.27**	**20.52**	**616.73**	**611.38**	**577.13**
Median 5x5	18.32	18.39	18.54	956.87	942.81	910.16
BM3D 0.2	4.20	4.37	4.47	24749.45	23795.33	23256.53
BM3D 0.4	4.20	4.37	4.47	24746.57	23790.29	23255.06

** Only Sentinel data with better results are shown in Table due to page restriction.*

(b)

Table 2. Statistical analysis of denoised Sentinel 2 image in the spatial domain for (a) homogeneous and (b) heterogeneous areas.

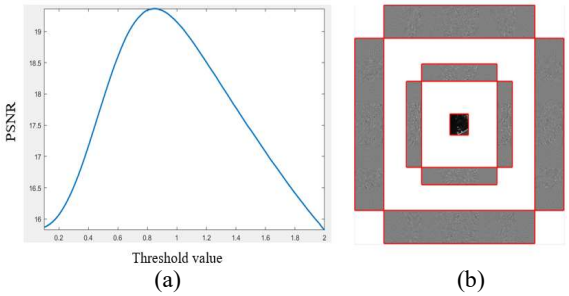

Figure 5. Example of (a) PSNR-threshold value graph and (b) Curvelet transform image.

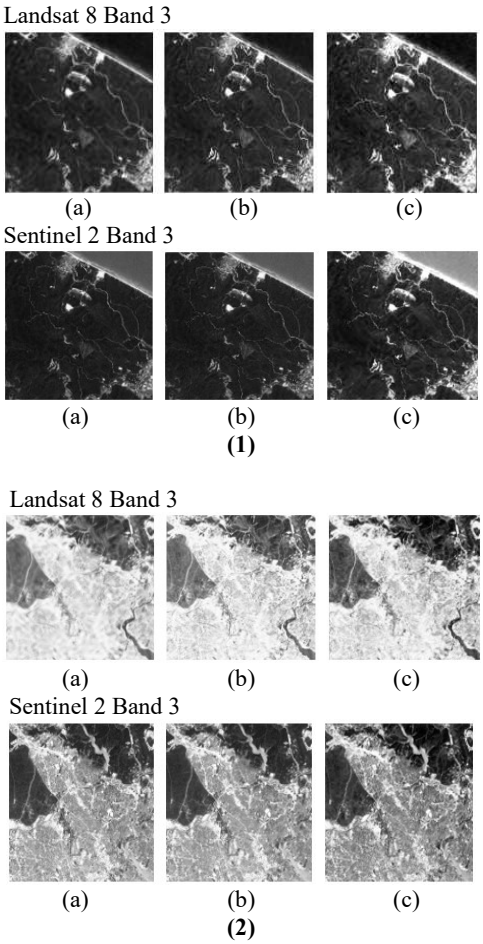

Figure 6. Denoised images of test areas on Landsat 8 and Sentinel 2 images for (1) homogeneous and (2) heterogeneous areas; (a) Curvelet soft thresholding, (b) Curvelet hard thresholding, (c) Contourlet.

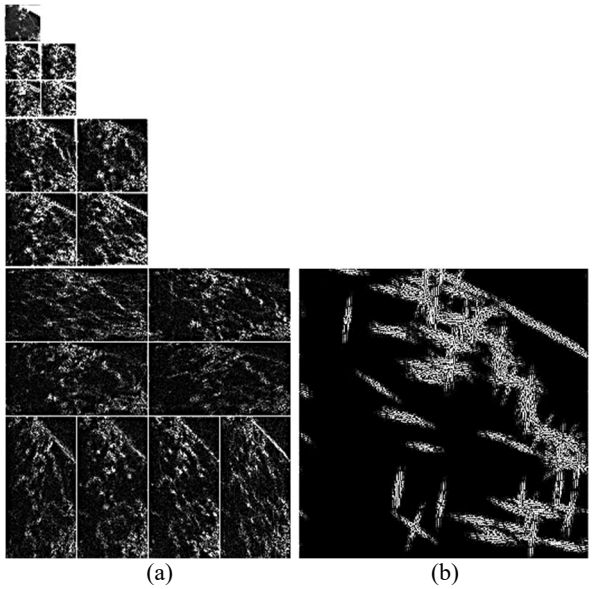

Figure 7. Example of Contourlet transform subbands for homogeneous area in the Band 2 image of Sentinel 2 (a) σ=10 Gaussian noise in the subbands and (b) zoomed-in view of one of the subbands (small coefficients are shown in black and large coefficients are shown in white).

Landsat 8	PSNR				MSE			
	B2	B3	B4	B8	B2	B3	B4	B8
σ=10 Gaussian Noise								
Curvelet Soft Threshold	27.10	26.43	26.65	26.92	126.68	147.97	140.65	132.15
Curvelet Hard Threshold	**31.29**	**31.35**	**31.37**	**30.93**	**48.28**	**47.66**	**47.66**	**52.44**
Contourlet	28.63	27.95	28.07	28.48	89.20	104.26	101.33	92.35
σ=20 Gaussian Noise								
Curvelet Soft Threshold	22.40	21.36	21.94	22.02	373.98	475.22	415.89	408.04
Curvelet Hard Threshold	**24.99**	**24.53**	**24.83**	**24.54**	**206.29**	**229.26**	**213.76**	**228.80**
Contourlet	24.22	23.15	23.75	23.82	246.02	315.08	274.12	270.08

(a)

Landsat 8	PSNR				MSE			
	B2	B3	B4	B8	B2	B3	B4	B8
σ=10 Gaussian Noise								
Curvelet Soft Threshold	25.28	25.30	25.42	26.92	192.94	192.07	186.50	132.15
Curvelet Hard Threshold	**32.85**	**32.77**	**32.57**	**30.93**	**33.76**	**34.35**	**35.98**	**52.44**
Contourlet	26.80	26.56	26.58	26.29	135.87	143.48	143.00	152.84
σ=20 Gaussian Noise								
Curvelet Soft Threshold	20.44	20.45	20.55	22.02	587.26	586.41	572.48	408.04
Curvelet Hard Threshold	**25.07**	**25.04**	**24.99**	**24.54**	**202.56**	**203.76**	**205.93**	**228.80**
Contourlet	22.79	22.60	22.60	22.37	341.86	357.66	357.50	376.42

** Only Landsat data with better results are shown in Table due to page restriction.*

(b)

Table 3. Statistical analysis of denoised Landsat 8 image in the spatial domain for (a) homogeneous and (b) heterogeneous areas.

4.4 Stripe noise denoising in the spatial domain

All denoising methods were also tested on satellite images with stripe noise.

In the Median filter application, the kernel selection was effective as in the Gaussian noise. The use of a 5x5 kernel resulted in a smoother denoised image than a 3x3 kernel, but neither of these methods was able to effectively remove stripe noise (Figure 8(a) and Figure 8(b)).

The images denoised with BM3D method showed that this method also did not gave good results in stripe noise adequately. It can be seen from Figure 8(c) and Figure 8(d) that both the main features in the images such as settlements are blurred and the stripe noise cannot be completely eliminated.

The statistical results showed that Median filter with a 3x3 kernel gave better results than other three methods (with higher PSNR value, Table 4)).

4.5 Stripe noise denoising in the frequency domain

In contrast to the methods used in the spatial domain (especially the Median filter), the methods chosen in the frequency domain gave worse results in removing the stripe noise.

In the output images obtained, various artifacts were also seen in both methods (Curvelet and Contourlet), as in Gaussian noise, and stripe noise cannot be eliminated (Figure 9).

According to the statistical analysis on the denoising methods used for the stripe noise images, the Curvelet transform with hard thresholding gave the best result with the highest PSNR value. However, stripe noise could not be eliminated by any method applied in the frequency domain (Table 5).

Overall, the Median filter with a 3x3 kernel in the spatial domain and Curvelet transform with hard thresholding in the frequency domain were selected as the best methods for removing or suppressing Gaussian and stripe noises in both satellite images.

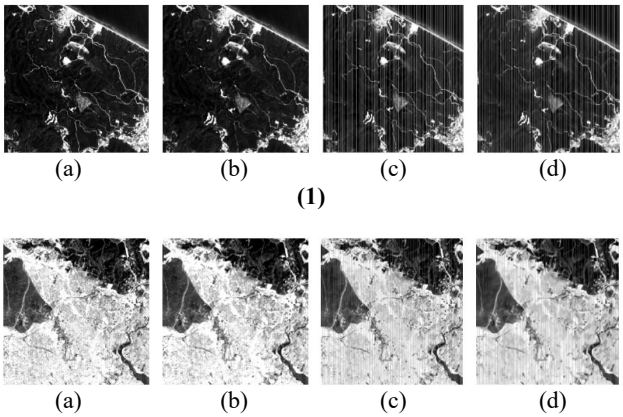

Figure 8. Denoised images of test areas on Landsat 8 images with stripe noise for (1) homogeneous and (2) heterogeneous areas; (a) Median 3x3 filter, (b) Median 5x5 filter, (c) σ=0.2 BM3D, (d) σ=0.4 BM3D.

Method	PSNR		MSE	
	Homogeneous Test Area	Heterogeneous Test Area	Homogeneous Test Area	Heterogeneous Test Area
Median 3x3	**13.30**	**18.65**	**3044.00**	**888.18**
Median 5x5	12.89	17.11	3340.30	1264.05
BM3D 0.2	3.88	1.87	26594.67	42295.70
BM3D 0.4	3.88	1.87	26595.44	42297.83

Table 4. Statistical analysis of denoised Landsat 8 panchromatic image in the spatial domain for stripe noise.

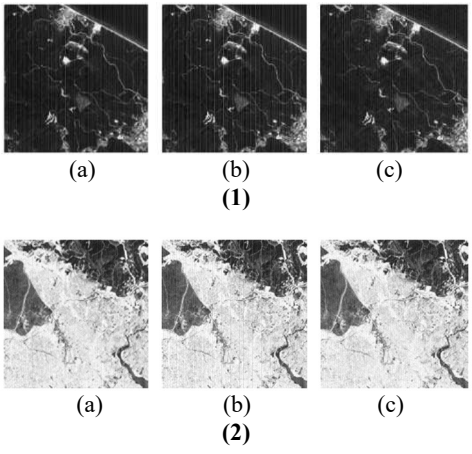

Figure 9. Denoised images of test areas on Landsat 8 images with stripe noise for (1) homogeneous and (2) heterogeneous areas; (a) Curvelet soft thresholding, (b) Curvelet hard thresholding, (c) Contourlet.

Method	PSNR		MSE	
	Homogeneous Test Area	Heterogeneous Test Area	Homogeneous Test Area	Heterogeneous Test Area
Curvelet Soft Threshold	24.03	21.42	256.85	468.65
Curvelet Hard Threshold	**30.61**	**26.38**	**56.51**	**149.68**
Contourlet	23.93	21.26	262.90	429.26

Table 5. Statistical values of denoising algorithms in the frequency domain for stripe noise.

5. CONCLUSION

Denoising is one of the hot research topics and has evolved continuously since the beginning of image processing. Studies are generally on test images, but in this study, four different denoising methods were examined using Landsat 8 and Sentinel-2 images and evaluated by statistical quality measures such as PSNR, MSE, standard deviation, and min/max values.

First of all, it was found that spatial resolution generally affects and improves the visual quality of the denoised image.

It was observed that both methods used in the spatial domain, namely Median and BM3D, cause data loss as the most important drawback. According to the quality analysis, the statistical values of the Median filter were found to be better than BM3D for two different densities of Gaussian noise in both satellite images (denoised image by using Median filter has 50% higher PSNR than BM3D in the homogeneous test area while almost 90% higher PSNR in the heterogeneous test area). Although the statistics show that the Median filter is better than BM3D, it has been visually observed that the noise in the images does not completely disappear.

On the other hand, in the frequency domain, it was observed that the fine details of the image are preserved, but some artifacts occur for Gaussian noise denoising in both images. Also, different thresholding values increased the performance of Curvelet. In addition, statistical values obtained with Curvelet hard thresholding are better than Curvelet soft thresholding and Contourlet (denoised image by using Curvelet hard threshold has 10% higher PSNR than soft threshold and Contourlet). After all, when all algorithms (Median, BM3D, Contourlet and Curvelet) were compared to each other, Curvelet hard thresholding was found to be better visually and statistically.

For stripe noise, the performance of all algorithms was not found to be effective compared to Gaussian noise.

As a final result, although some methods in both domains show higher performance than others, the methods used for denoising need to be tested in other test areas or with other image datasets in order to generalize. For this reason, as a future study, it is planned to evaluate their effectiveness and applicability on image quality by using various noise removal techniques both in different satellite images and in test areas.

ACKNOWLEDGEMENT

We are very thankful to Minh Do for providing the Contourlet Toolbox and Emmanuel Candes and his friends for sharing the CurveLab software package. We are also grateful to Turkish Aerospace Industries (TAI) for helpful discussions and motivational support from the beginning of the study.

REFERENCES

Ahmed, E.S.A., Elatif, R.E.A., Alser, Z.T., 2015. Median Filter Performance Based on Different Window Sizes for Salt and Pepper Noise Removal in Gray and RGB Images. *8*, 343-352. doi.org/10.14257/ijsip.2015.8.10.34

Altun, A.A., Allahverdi, N., 2007. A New Approach to Recognition of Fingerprints Enhanced by Filtering Techniques with Artificial Neural Networks (in Turkish). *Journal of Gazi University Faculty of Engineering and Architecture, 2*, 227-236.

Dabov, K., Foi, A., Katkovnik, V., Egiazarian, K., 2007. Image Denoising by Sparse 3-d Transform-Domain Collaborative Filtering. *IEEE Transactions on Image Processing*, *16*(8), 2080-2095. doi.org/10.1109/TIP.2007.901238

Do, M.N., Vetterli, M., 2005. The Contourlet Transform: An Efficient Directional Multiresolution Image Representation. *IEEE Transactions on Image Processing*, *14*(12), 2091-2106. doi.org/10.1109/TIP.2005.859376

Lebrun, M., 2012. An Analysis and Implementation of the BM3D Image Denoising Method. *Image Processing On Line*, *2*, 175-213. doi.org/10.5201/ipol.2012.l-bm3d

Luisier, F., Blu, T., Unser, M., 2007. A New Sure Approach to Image Denoising: Interscale Orthonormal Wavelet Thresholding. *IEEE transactions on image processing : a publication of the IEEE Signal Processing Society*, *16*, 593-606. doi.org/10.1109/TIP.2007.891064

Naveed, K., Shaukat, B., Ehsan, S., Mcdonald-Maier, K.D., Ur Rehman, N., 2019. Multiscale Image Denoising Using Goodness-of-Fit Test Based on EDF Statistics. *PLOS ONE*, *14*(5), 1-25. doi.org/10.1371/journal.pone.0216197

Nencini, F., Garzelli, A., Baronti, S., Alparone, L., 2007. Remote Sensing Image Fusion Using the Curvelet Transform. *Information Fusion*, *8*(2), 143-156. doi.org/10.1016/j.inffus.2006.02.001

Rajkumar, S., Malathi, G., 2016. A Comparative Analysis on Image Quality Assessment for Real Time Satellite Images. *Indian Journal of Science and Technology*, *9*. doi.org/10.17485/ijst/2016/v9i34/96766

Ruikar, S.D., Doye, D.D., 2011. Wavelet Based Image Denoising Technique. *International Journal of Advanced Computer Science and Applications, 2(3).* doi.org/10.14569/IJACSA.2011.020309

Sunar, F., Ozkan, C., Ok, A.O., Osmanoglu, B., Avci, Z., Berberoglu, S., (2017). Digital Image Processing (in Turkish), Anadolu University press, Eskişehir

Tsai, F., Chen, W.W., 2008. Striping Noise Detection and Correction of Remote Sensing Images. *IEEE Transactions on Geoscience and Remote Sensing*, *46*(12), 4122-4131. doi.org/10.1109/TGRS.2008.2000646

Vijay, M.M., Devi, L.S., 2012. Speckle Noise Reduction in Satellite Images Using Spatially Adaptive Wavelet Thresholding.

Wang, Z., Bovik, A.C., 2006. Modern image quality assessment. *Synthesis Lectures on Image, Video, and Multimedia Processing*, *2*(1), 1-156.

Yu, H., Zhao, L., Wang, H., 2009. Image Denoising Using Trivariate Shrinkage Filter in the Wavelet Domain and Joint Bilateral Filter in the Spatial Domain. *IEEE Transactions on Image Processing*, *18*(10), 2364-2369. doi.org/10.1109/TIP.2009.2026685